The effect of a living wall system designated for greywater treatment on the hygrothermal performance of the facade

Hayder Alsaad*, Maria Hartmann, Conrad Voelker

Bauhaus-University Weimar, Department of Building Physics
Coudraystrasse 11A, Room 110
99423 Weimar, Germany
**Corresponding author: hayder.alsaad@uni-weimar.de*

(Received 16 September 2021, Revised 4 November 2021, Accepted 19 November 2021)

Abstract

Besides their multiple known benefits regarding urban microclimate, living walls can be used as decentralized stand-alone systems to treat greywater locally at the buildings. While this offers numerous environmental advantages, it can have a considerable impact on the hygrothermal performance of the facade as such systems involve bringing large quantities of water onto the facade. As it is difficult to represent complex entities such as plants in the typical simulation tools used for heat and moisture transport, this study suggests a new approach to tackle this challenge by coupling two tools: ENVI-Met and Delphin. ENVI-Met was used to simulate the impact of the plants to determine the local environmental parameters at the living wall. Delphin, on the other hand, was used to conduct the hygrothermal simulations using the local parameters calculated by ENVI-Met. Four wall constructions were investigated in this study: an uninsulated brick wall, a precast concrete plate, a sandy limestone wall, and a double-shell wall. The results showed that the living wall improved the U-value, the exterior surface temperature, and the heat flux through the wall. Moreover, the living wall did not increase the risk of moisture in the wall during winter and eliminated the risk of condensation.

1. Introduction

Around the globe, there is a growing demand for buildings for commercial and non-commercial purposes. This is due to the worldwide constant growth of population along with a rising trend to more mobilisation leading to a fast increase in the built and paved areas in the cities with a simultaneous decrease in green areas in the urban environment. This reduction in city greenery kindles decreased residents' mental and physical wellbeing, increased air pollution levels, and a rising air temperature due to the urban heat island effect.

Facade greening has been growingly investigated as a practical solution to expand the urban greenery, and subsequently improve the urban environment. The literature distinguishes two variations of facade greening systems based on their growing method: green facades and living walls. The first type, green facades, refers to greenery planted in the ground -or in planting containers on the ground- that grows on or in front of the facade. On the other hand, a living wall consists of substrate boxes or trays mounted on the facade to provide a growing medium for the roots [1]. The benefits of both systems have been frequently investigated in the literature. Among other benefits provided by facade greening such as improved air quality, biodiversity, crop production, etc., the thermal effect of wall greening systems has been the centre of focus [2]. This effect includes the cooling potential of the systems during the hot season as well as the possibly added external insulation in the cold season [3]. Susorova et al. [4] developed a mathematical model to assess the impact of greenery on heat transfer through the wall. They illustrated an improvement in thermal resistance of up to 0.7 m^2K/W. Tudiwer and Korjenic [5] implemented empirical measurements to evaluate the impact of living walls on the thermal resistance of the facade. They found that the greening system increased the facade's thermal resistance by 0.31–0.67 m^2K/W. Wong et al. [6] recorded the effects of eight wall greening systems on the ambient temperature. They observed different patterns depending on the greenery system. Their results ranged from a hardly noticeable impact on air temperature to a cooling effect reaching 0.6 m from the system. They argued that this can lead to a reduced air temperature in the street canyon, which translates into a reduced air temperature at the air-conditioning intake leading to energy savings. Perini et al. [3] measured air velocity at multiple points within and in front of different facade greening systems. Their measurements showed a reduced wind velocity in front of the wall indicating a reduced exterior surface resistance R_{se}. Moreover, their surface temperature measurements confirmed that the greening systems can act as natural sunscreens for the reduction of facade surface temperature in summer. This agrees with the results illustrated in [7], which indicate that the surface temperature on the living wall in the summertime ranged between 12.5–46°C compared to 14–61°C on the bare wall. Cheng et al. [8] reported a delayed solar heat transfer into the building when greening is used, and thus reduced cooling energy requirements compared to a concrete wall with no greening. Chen et al. [9] suggested that a sealed air layer behind the living wall yielded a better cooling effect compared to a naturally ventilated air gap. Furthermore, they reported a high cooling effect on the exterior wall up to 20.8 K which led to a reduction in the interior surface temperature and room air temperature by up to 7.7 K and 1.1 K respectively. Similar results were shown by Safikhani et al. [10], who indicated a reduced indoor air temperature by 4 K and 3 K when a living wall and a green facade were implemented, respectively. Cuce [11] conducted numerical assessments in addition to experimental investigation and reported a promising average of 2.5 K reduction in interior wall temperature when a green wall with climbing ivy (hedera helix) is used.

Besides the thermal benefits of the living walls, they have been studied as a potential treatment system for greywater produced in the building to mitigate the handling load on water treatment centres. The targeted greywater includes drain water from the kitchen and the bathroom except for wastewater from the toilet, i.e. wastewater released from sinks, dishwashers, washing machines, showers, and bathtubs. The treated greywater could be then used as a substitute for potable water for irrigation or toilet flushing [12]. Aicher and Londong [13] reported that implementing mineral wool cubes as a substrate for the living wall showed good potential for purification and nitrification rates. Prodanovic et al. [14] also explored the efficiency of several types of hydraulically slow and fast media and their treatment potential. They suggested that perlite has the best purification and hydraulic performance compared to the other tested media. Masi et al. [15] tested a living wall with lightweight expanded clay aggregate (LECA) mixed with either sand or coconut fibres as a substrate for greywater treatment. They reported a chemical oxygen demand removal of 7–80% for LECA+sand and 14–86% for LECA+coconut fibres. Wolcott et al. [16] investigated the potential of using living walls with recycled glass media as a substrate to pre-treat wastewater from small to medium-sized breweries. Their results indicated a 65% reduction of biochemical oxygen demand after a 24-hour treatment time. Besides the choice of substrate, the literature indicates that the utilized plants play an important role in pollutant removal as well [17].

While living walls designated for greywater treatment offer promising environmental advantages, they involve bringing large quantities of water to the facade. Even though living walls typically have a ventilated air gap separating them from the wall construction, they can still increase the humidity level in the wall [18]. This is due to evaporation from the substrate and transpiration from the plants combined with low outside air temperatures. An increase in humidity can damage the building material and reduce the energy efficiency of the building by increasing the heat conductivity of the wall layers. Moreover, moisture in building components can result in adverse health issues due to, among others, mould growth [19].

As hygrothermal simulations of facades equipped with living walls for greywater reuse are not reported in the literature, this study aims to numerically investigate the heat and moisture transport in such systems. The goal is to explore the impact of relatively high exposure to moisture on the facade. Since the impact of the living wall depends on the wall construction behind it, four different wall assemblies were simulated in this study. Multiple hygrothermal parameters were simulated and assessed. Moreover, the impact of the living wall on the thermal transmittance of the wall (U-value) was calculated.

2. Methods

As most heat and moisture simulation models cannot simulate the complex impact of vegetation on the physical parameters at the facade, this study was conducted by coupling two simulation tools: ENVI-Met and Delphin [20]. ENVI-Met is a high-resolution meteorological model that can simulate the interaction between urban geometry, vegetation, and the outdoor environment [21]. Delphin, on the other hand, is a simulation package for coupled heat and moisture transport in capillary porous building materials [22]. Both simulation models are frequently used in literature; their validation can be found in numerous studies such as Salata et al. [23] and Sontag et al. [24]. In the present study, ENVI-Met was used to calculate the influence of the plants on air temperature, velocity, relative humidity, wind direction, and radiation (long wave and short wave) at the living wall. Thus, ENVI-Met was used to determine the local climate conditions at the facade based on the global weather data in the investigated site. Subsequently, the calculated local climate conditions were imposed as exterior boundary conditions in Delphin to conduct the hygrothermal simulations (Figure 1). The local climate data included the wind direction in front of the living wall, the air temperature, air velocity, and relative humidity in the foliage of the living wall, and the total short-wave and long-wave radiation received by the surface behind the foliage. The driving rain was not simulated in ENVI-Met. Instead, it was assumed that no liquid water was penetrating the foliage. Therefore, in the local weather data implemented in Delphin, the driving rain reaching the substrate behind the foliage was set to zero.

The simulated living wall corresponds to the greywater treatment system developed at the Bauhaus-University Weimar, Germany [25]. The system consists of metal planting boxes mounted on a metal frame erected in front of the facade. The distance between the system and the facade wall is about 50 mm; this space comprises a highly-ventilated air gap. The planting boxes are 0.5 x 0.4 x 0.25 m (L x H x D). The backside of the boxes is a rigid 12 mm polyethylene (PE) plate. The front side of the system is covered with flexible cotton-based textile that retains water and odours; holes are punctured in the textile to plant the plants horizontally in the growing medium. The boxes are stacked on top of each other according to the desired height for the living wall; multiple columns of boxes can be arranged next to each other according to the size of the facade. The volume of the substrate in this developed system is 150 L/module, in which a living wall module consists of three stacked planting boxes. Various growing media can be used depending on their efficiency in greywater treatment. In the simulations presented in this study, the implemented substrate consisted of a mixture of expanded clay aggregate (66.6%) and biochar (33.3%). The designed greywater treatment capacity is one module for each resident in the building with the assumption that each resident generates 75 L/d of greywater [25]. This value represents a rough average as greywater production can range from 15 to several hundred litres per resident per day, depending on the region [26]. The greywater is supplied into the system through the top planting boxes; the greywater then flows through the boxes until reaching a collection trough underneath the system from which the treated water is pumped into a storage tank for later use as irrigation water.

To evaluate the impact of the living wall, two scenarios were simulated: a facade covered with a living wall and a reference facade with no greening (bare wall). The simulated facade was oriented south and located in Mannheim, Germany. This city was selected for the simulations as it lies in the German climate region C which is characterized by warm temperatures in the summer [27]. The weather data for the simulations were adopted from the test reference year (TRY) data provided by the German weather service (DWD).

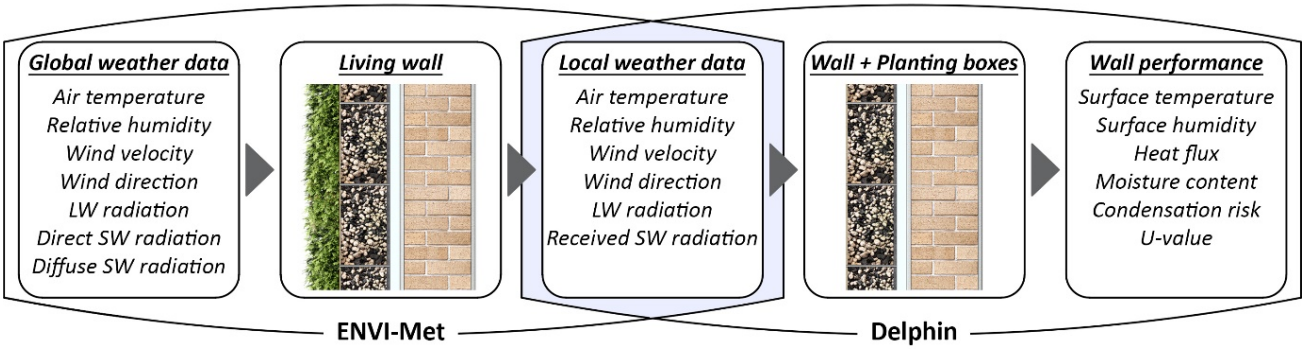

Figure 1. The coupling of ENVI-Met and Delphin

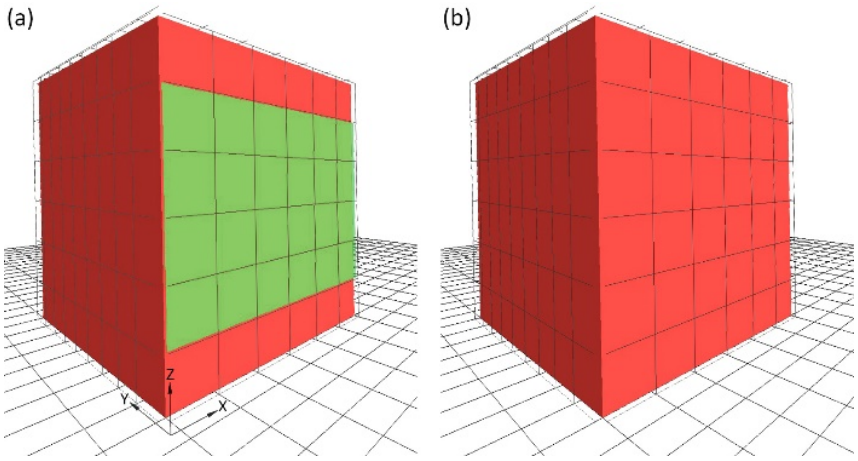

Figure 2. The geometry of ENVI-Met models; (a) with greening, (b) no greening (the reference case)

2.1. ENVI-Met model

ENVI-Met 4.4 was implemented to simulate the local climate on the facade using a 3D geometry of a simple test container with the size of 4.5 x 4.5 x 4.5 m. The container was situated at the centre of a 22.5 x 22.5 x 20 m computation domain. This provided sufficient distance between the surfaces of the container and the edges of the domain of 2H at the sides and 3H at the top according to the recommendations of ENVI-Met [28]. The domain was discretised with a 0.75 x 0.5 x 0.75 m grid (dx, dy, dz). The grid cells on the Y-axis (dy) were set to the smallest possible grid size in ENVI-Met (0.5 m) in order to ensure a fine resolution in front of the greening system. To reduce the total number of cells, the grid size was telescopically increased in the vertical direction with a growth rate of 20% starting from the second cell above the container (at 5.25 m). In total, the domain consisted of 20250 cells.

Two geometries were created for the ENVI-Met simulations: with and without greening (Figure 2). To reduce the computation time, both geometries implemented a generic wall construction (d = 410 mm). In the living wall simulation scenario, a 4.5 x 3 m living wall was modelled on the south-facing facade (XZ plane). The construction of this living wall corresponded to the details and dimensions of the greywater treatment system reported in the Methods section. To capture a scenario with high transpirational moisture generation, the leaf area density (LAD) index of the plants in the living wall was set to 6 m^2/m^3 according to the values reported for facade greening shrubs [29]. To accommodate the changes in the leaf density through the seasons of the year, an LAD profile was created in which the LAD in the summer months is 50% higher than in the winter months. It is important, however, to point out, that this profile is nothing but a rough estimation of the changes that evergreen plants encounter throughout the seasons of the year. It is solely implemented to take the changes in LAD into consideration. In reality, these changes depend on numerous factors such as plant type, orientation, solar radiation, irrigation, etc., and therefore, no LAD profile can be generalized or drawn from the literature. Further parameters that were used to represent the plants in this study included a canopy albedo of 0.3, a transmittance index of 0.2, and a leaf angle distribution of 0.25.

The simulations were conducted with a time step of 2 s at the initialization and 1 s throughout the rest of the simulations. Since the goal of ENVI-Met simulations was to calculate the local climate data for the hygrothermal simulations, the simulations were conducted for a time span of one year with hourly data output. To avoid influencing the near-facade boundary conditions, the indoor temperature in the ENVI-Met model was defined as a variable based on the exterior conditions, i.e. no active heating or cooling were implemented. The lateral boundaries were defined using the so-called full-forcing approach, in which the values of air temperature, wind speed, wind direction, short-wave and long-wave radiation, and relative humidity were assigned to the inflow boundary in 30-minute time steps based on the hourly values taken from the TRY weather file. The simulations were conducted using the standard k-e turbulence model with 1.5 order turbulence closure. Extra source terms are defined in the transport equations of momentum and turbulence to accommodate the impact of vegetation on the flow. Full details about the mathematical principles of ENVI-Met can be found in Huttner [30].

2.2. Delphin model

Delphin 6 was implemented to conduct 1D heat and moisture transport simulations of the tested living wall system. To investigate the impact of greening on different types of constructions, four wall assemblies were simulated: an uninsulated brick wall, a precast concrete building plate, a sandy limestone wall, and a double-shell wall. These assemblies were selected based on the construction types common in Germany [31,32]. Tables 1 and 2 present the wall construction of these assemblies and the physical properties of the building materials for the simulated walls, respectively. The implemented material properties are taken from the Delphin material database and the MASEA databank of German building material [33].

Table 1. Wall construction of the investigated wall assemblies. The layers are listed from interior to exterior

Wall assembly	Layers	Thickness [mm]
Uninsulated brick wall	Gypsum plaster	15
	Full bricks	380
	Lime plaster	15
Precast concrete plate	Concrete	150
	EPS	40
	Concrete	60
Sandy limestone wall	Gypsum plaster	15
	Sandy limestone	240
	EPS	80
	Lime plaster	15
Double-shell wall	Gypsum plaster	15
	Porous concrete	175
	Mineral wool	100
	Veneer bricks	90

Similar to ENVI-Met simulations, two Delphin simulation models were created (Figure 3). In the reference case (without greening), the exterior surface of the simulated construction was the exterior layer of the wall. In the living wall scenario, the construction included three additional layers in front of the wall: air gap, PE-plate, and substrate boxes. Thus, in this case, the substrate boxes were the exterior surface of the assembly. The flexible textile covering the front-side of the substrate boxes was not explicitly modelled. Instead, its hygrothermal impact was included in the model by adding an extra vapour diffusion thickness (s_d-value) of 0.1 m to the exterior surface. This low value was chosen to account for the vapour permeability of the textile as well as the holes in which the plants were planted.

The created Delphin models had the same orientation as the ENVI-Met models. Each simulated wall assembly had a height of 100 cm; the geometry was discretised with elements ranging from a minimum size of 1 mm to a maximum size of 50 mm with a growth factor of 1.3. Detailed exterior and interior boundary conditions were imposed on the left and right sides of the geometry. The parameters of the exterior boundary conditions, as mentioned in the Methods section, corresponded to the local climate parameters simulated with ENVI-Met. For the calculation of heat exchange between the exterior surface and the outdoor environment, a variable convective heat transfer coefficient h_c [W/m²K] was defined as a function of the outdoor hourly air velocity v [m/s] according to:

$$h_c = h_{c0} + k_h \cdot v^{kexp} \quad (1)$$

Where h_{c0} is the transfer coefficient for still air [W/m²K], k_h is the slope coefficient for moving air [J/m³K], and k_{exp} is the exponent for moving air [-]. Similarly, the water vapour exchange coefficient β [s/m] was defined as a variable as well:

$$\beta = \beta_0 + k_v \cdot v^{kexp} \quad (2)$$

Where β_0 is the exchange coefficient for still air [s/m], k_v is the slope coefficient for moving air [s²/m²] and k_{exp} is the exponent for moving air [-].

As for radiation, the short-wave radiation (0.2 µm to 3 µm) on the exterior surface was defined as imposed flux oriented to the wall. The absorption coefficient for short-wave radiation differed between the 'no greening' and the 'with greening' cases. For the 'no greening' case, an absorption coefficient of 0.6 was set corresponding to a muted exterior colour. For the 'with greening' case, this value was set to 0.4 to simulate the light-coloured textile used to cover the front face of the

Table 2. The material properties implemented in the hygrothermal simulations

Material	Density ρ [kg/m³]	Porosity ϕ [m³/m³]	Vapour resistance μ [-]	Heat capacity c [J/kgK]	Conductivity λ [W/mK]	Water uptake Aw [kg/m²s$^{0.5}$]
Gypsum plaster	1043	0.606	11.3	1047	0.26	0.366961
Full bricks	1790	0.360	14	868	0.87	0.227000
Lime plaster	1270	0.500	12	960	0.55	0.009300
Concrete	2320	0.143	63	850	2.10	0.008333
EPS	35	0.935	50	1500	0.04	0.000010
Sandy limestone	1744	0.359	27.9	850	0.82	0.049673
Porous concrete	415	0.832	8.9	850	0.10	0.039065
Mineral wool	37	0.920	1	840	0.03	0.000001
Veneer bricks	1852	0.301	27.1	810	0.68	0.040674

substrate boxes. Similar to short-wave radiation, long-wave radiation (4 μm to 40 μm) was defined as an imposed flux normal to the surface. The emission coefficient of the exterior surface in both simulated cases (with and without greening) was set to 0.9. To calculate the liquid water flux on the exterior surface, the driving rain model from the DIN EN ISO 15927-3 [34] was implemented. For the reference case with no greening, the precipitation values in L/m²h were taken directly from the test reference year data. On the other hand, in the 'with greening' case, the precipitation was set to zero with the assumption that no liquid water was reaching behind the foliage as discussed in the Methods section.

The interior boundary conditions corresponded to the adaptive indoor climate model defined by the DIN EN 15026 [35] and the Association for Science and Technology of Building Maintenance and Monuments Preservation (WTA) [36]. This model calculates the daily mean indoor air temperature and relative humidity based on the value of the daily mean outdoor temperature (Figure 4, a). The so-called Normal+5% model for the indoor air humidity was utilized, which includes a safety margin of an additional 5% to the indoor relative humidity to accommodate local increases in humidity resulting from specific usage of the room behind the facade (e.g. a kitchen or a bathroom). Thus, this model prevents underestimating the indoor relative humidity when the function of the room is unknown. The default values of the indoor air temperature range of 20–25°C and the indoor relative humidity range of 35–65% were implemented. An

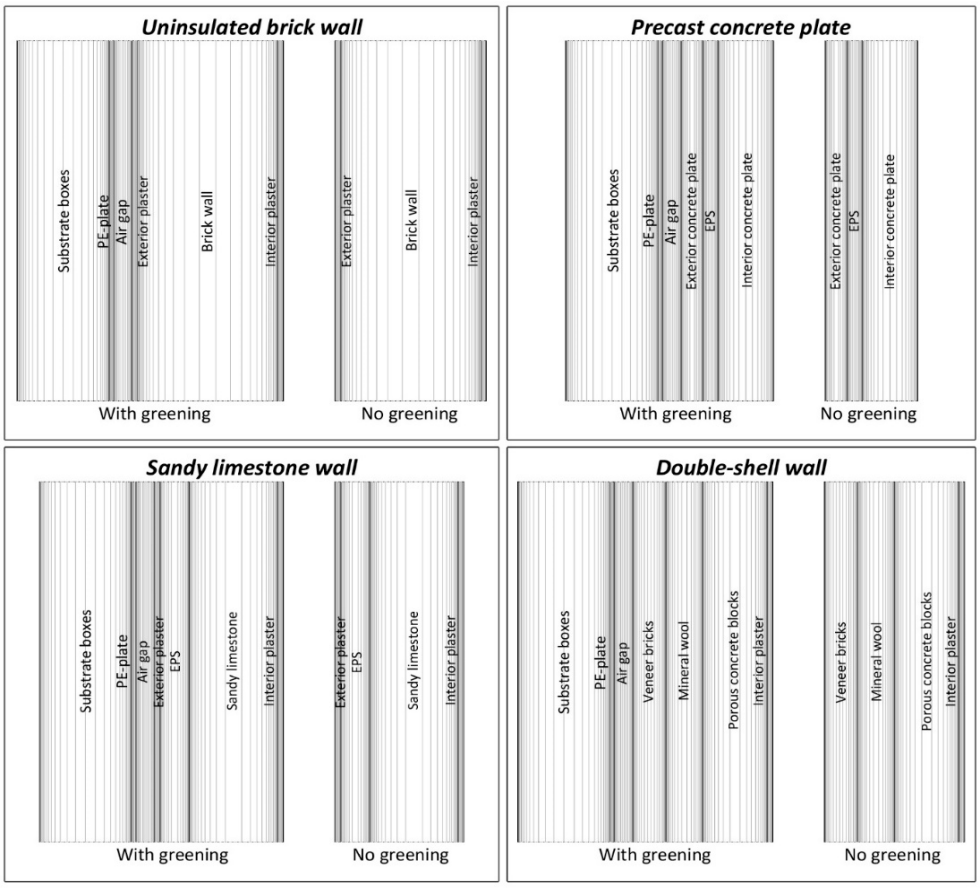

Figure 3. The geometry of the Delphin models

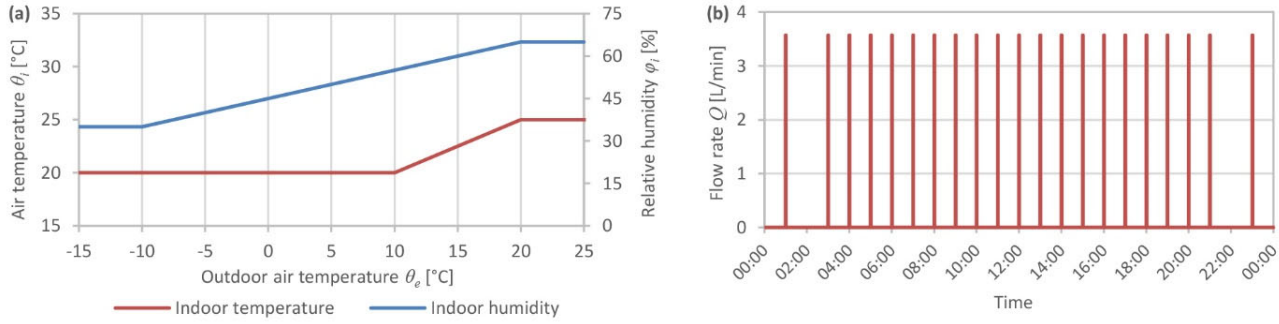

Figure 4. (a) The indoor air temperature and relative humidity in relation to the outdoor air temperature [36]; (b) The daily greywater supply cycle implemented in the simulations

indoor heat transfer coefficient of 8 W/m²K was assigned to the indoor surface to consider both convective and radiative heat transfer. The surface vapour diffusion coefficient was set to 2.5e-08 s/m.

In the living wall scenario, a 50 mm ventilated air gap was positioned between the wall and the substrate boxes. To represent air exchange with the outdoor air, an air change rate was defined in the gap. The value of the change rate was set to 20/h corresponding to a highly-ventilated gap located within a city with average shielding by surrounding buildings [37]. The temperature and relative humidity of the incoming air was equivalent to the hourly values of the local climate parameters and was updated at each time interval of the simulation. To simulate the long-wave radiative heat exchange between the two sides of the air gap, i.e. between the exterior surface of the wall and the back-side of the planting boxes, a radiative exchange source was defined in the gap with an emission coefficient of 0.9 on both sides. Moreover, the convective heat transfer coefficient between the wall and the air gap was set to 2.5 W/m²K, which corresponds to the transfer coefficient of calm air according to DIN EN ISO 6946 [38]. For the same reason, the water vapour exchange coefficient in this material-air contact region was set to 1.53e-08 s/m. Lastly, the air gap was assumed to be sheltered from the top and the sides. Therefore, no humidity source was defined in the air gap to account for liquid water from the driving rain reaching the wall behind the living wall.

To simulate the flow of greywater in the substrate, a simple liquid water source with a rate of 75 L/d was defined. To accurately capture the greywater flow pattern in the substrate, a water supply profile was created according to the operation time intervals of the greywater pumps as specified by the developers of the system [25]. In this time profile, the water was flowing in the module only during the first minute of each hour of the day. However, no water was supplied into the substrate at three points in the profile, namely at 10:00 pm, 00:00 am, and 02:00 am (Figure 4, b). These points were set to reduce the load on the pumps during the night hours when the evaporation rate and water demand of the plants are low.

The simulations were initiated with a default temperature of 20°C and a default relative humidity of 80%. The simulations were conducted with a time step of 5 s to avoid instabilities and a duration of four years to ensure reaching the equilibrium moisture content in the construction. The results presented in this study correspond to the simulated values during the fourth year of the simulation time with average hourly outputs. The relative tolerance of the solver was set to 1e-04 while the absolute tolerance for the moisture mass balance was set to 1e-06 to ensure high accuracy for the simulations.

2.3. U-value calculation

The U-value refers to the thermal transmittance of the building assembly. It indicates the amount of energy flowing through a square meter of the construction for each kelvin of temperature difference. The U-value is the typical criterion used for defining the minimum design requirement by different standards around the world, such as Germany's Passivhaus standard and Building Energy Law (GEG). It represents heat transfer in a steady-state (constant heat loss and constant temperature difference). It can be determined by empirical measurements over a longer period of time [39] or calculated based on the thermal conductivity, thickness, and geometry of each component in the building assembly [38]. The U-value can also be calculated using the outcome of hygrothermal simulations. In this case, it is defined as the 'effective' U-value as it includes the effect of the solar radiation and the infrared irradiation to the sky [40]. It is calculated as:

$$U_{\text{eff}} = \frac{\sum_{j=1}^{n} q}{\sum_{j=1}^{n} (\theta_{i,j} - \theta_{e,j})} \tag{3}$$

Where q is the heat flux [W/m²] and θ_i and θ_e are the indoor and outdoor air temperatures, respectively [°C]. While this equation is fairly simple, the challenge remains in selecting the output range whose average represents steady-state. In this study, the data filtration proposed by Tudiwer et al. [5] was implemented to determine this range. The first applied filter was that the heat flux must be larger than 0 to ensure removing the values of warm summer days from the data set. To ensure having a large temperature difference between the indoor and outdoor air, the second filter was having an average temperature difference of above 10 K within the prior 24 hours and never below 0 K within the prior 24 hours. The third filter was eliminating data with fluctuations larger than 2 K within the prior 24 hours. This applies to the temperature of indoor air, indoor surface, outdoor air, and outdoor surface. This filter ensures a pseudo steady-state by removing the impact of heat storage on the calculations.

Besides determining the effective U-value from the output of the hygrothermal simulations, the U-value was also calculated using the calculation method reported in the standard DIN EN ISO 6946 [38] using the equation:

$$U = \left(R_{si} + \sum_{j=1}^{n} \frac{d_j}{\lambda_j} + R_{se} \right)^{-1} \tag{4}$$

Where d [m] and λ [W/mK] are the thickness and thermal conductivity of each layer in the wall assembly, respectively. The R_{si} and R_{se} are the interior and exterior surface resistance [m²K/W], respectively. For the no greening cases, i.e. the bare walls, R_{si} was defined as 0.13 m²K/W while R_{se} was 0.04 m²K/W as specified in the standard for horizontal heat flow [38]. For the cases with greening, the construction components in front of the highly-ventilated air gap, specifically the components of the living wall, were not considered in the calculation of the U-value. Instead, both R_{si} and R_{se} were set to 0.13 m²K/W [38].

3. Results

3.1. Impact on local climatic data

At the living wall, the local weather parameters calculated by ENVI-Met illustrated the significant role that plants play in shaping the microenvironment. As presented in Figure 5 (a), the foliage remarkably reduced the wind speed in front of the planting boxes. Without greening, the air velocity at the bare wall was as high as 6.9 m/s. Yet it did not exceed 4.36 m/s in front of the substrate. The average local air velocity was 0.51 and 0.93 m/s with and without greening, respectively, corresponding to a velocity decrease of 45.2%. The impact of the plants on local air temperature was, nevertheless, not as significant (Figure 5, b). By transpirational cooling, the vegetation decreased the maximum air temperature within foliage by only 0.2 K in the summer months, and the average air temperature in both summer and winter were fairly similar. This could be attributed to constant air movement from the surroundings into the foliage, thus diminishing its impact on air temperature. Moreover, the small size of the simulated living wall also played a role on its limited influence on air temperature. The resulted marginal reduction in air temperature agrees with the values reported by Gromke et al. [41] who assessed the cooling effect of facade greening using CFD simulations.

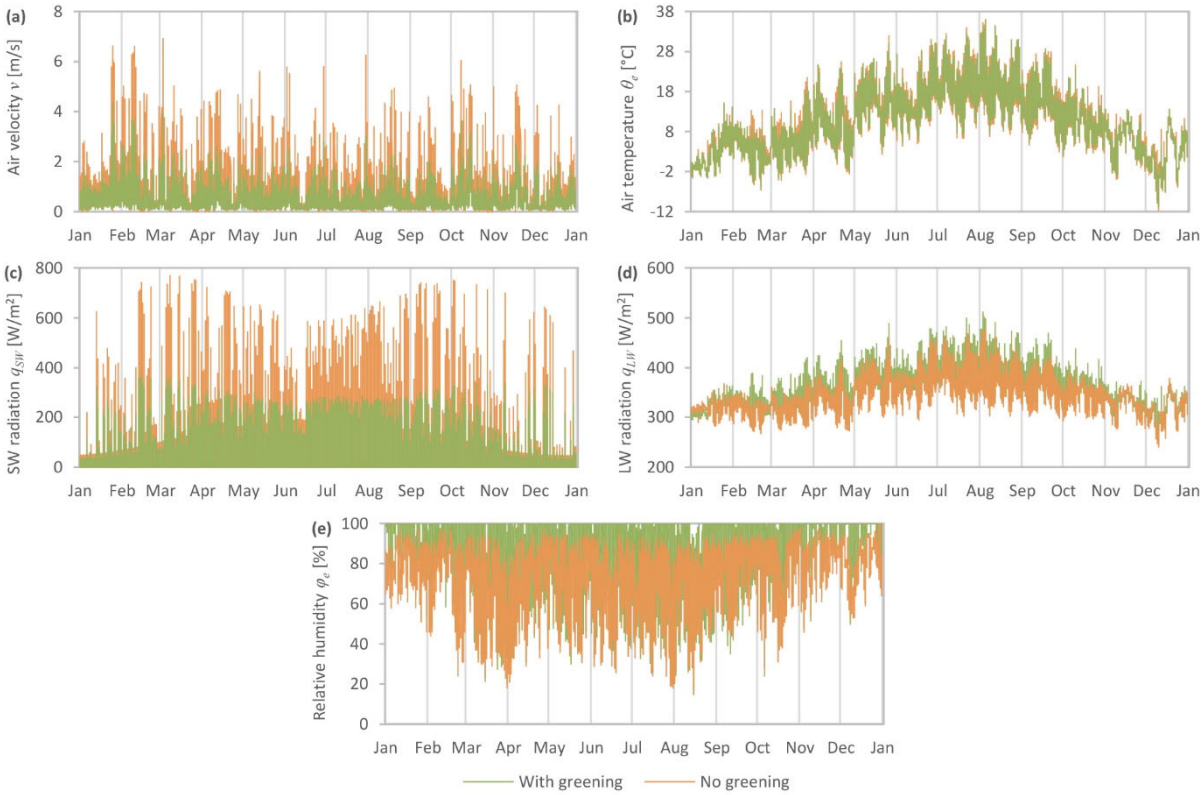

Figure 5. The local climatic data at the living wall determined by ENVI met. (a) Air velocity, (b) air temperature, (c) short-wave radiation, (d) long-wave radiation, and (e) relative humidity

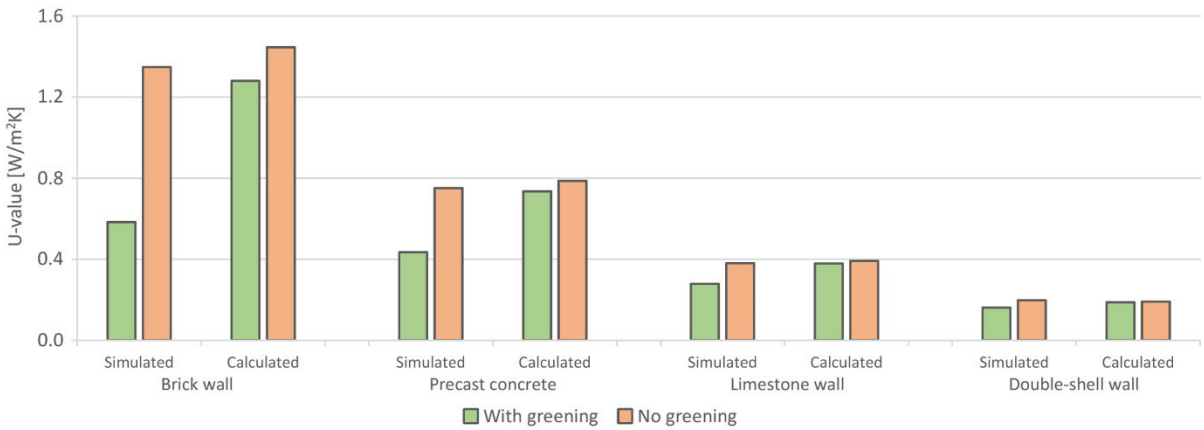

Figure 6. The simulated and calculated U-values of the investigated wall assemblies

The most considerable impact of the foliage can be observed in the values of the received short-wave radiation (Figure 5, c). While the bare wall received an average of 94.4 W/m^2, the substrate surface behind the foliage received only an average of 52.57 W/m^2. In other words, the foliage blocked an average of 44.3% of the solar radiation. The influence of the plants is most visible during the sunny days in which the blockage efficiency of the plants was up to 53.19%. It can also be noticed that the maximum received radiation was during the spring and autumn, not in the summer. This can be explained by the lower sun angle on the south facade. The received long-wave radiation illustrated a different pattern compared to the short-wave radiation (Figure 5, d). The reference facade with no greening received a maximum of 478.39 W/m^2 while the substrate surface received a maximum of 511.59 W/m^2. On average, the substrate surface received 2.3% more long-wave radiation in comparison to the bare wall. This can be explained due to the radiative exchange between the substrate surface and the relatively warm leaves in comparison to the exchange with the cold sky in the case of the bare wall. Similarly, the living wall increased the local relative humidity by an average of 15.1% and pushing the relative humidity to 100% in most of the simulated time (Figure 5, e). This increase is a result of transpiration from the leaves and evaporation from the substrate. Yet, as the German climate is already relatively humid, an even larger increase in humidity due to the living wall is likely to appear in dry arid climatic regions.

3.2. Impact on U-value

Figure 6 illustrates the effective U-value determined from the hygrothermal simulations (simulated) and determined according to the standard DIN EN ISO 6946 [38] (calculated). The results generally indicate that the living wall positively impacted the U-value of all the investigated walls. The worse the U-value of the bare wall, the higher the impact of the living wall. Thus, the U-value of the uninsulated brick wall showed the highest improvement of 0.77 W/m^{2}K. On the other hand, the improvement of the U-value of the highly insulated double-shell wall was only 0.04 W/m^{2}K.

The standard calculation resulted in fairly similar U-values of the bare wall compared to the simulated values. Nevertheless, the simulations showed that the standard calculation method tends to underestimate the benefit of the living wall. While the simulations method showed that greened uninsulated brick wall has a U-value of 0.58 W/m^{2}K, the calculation method yielded a remarkably lower value of 1.28 W/m^{2}K. The deviation between the simulation and calculation methods decreases as the U-value of the assembly improves. Hence, the difference between the simulated and calculated U-value of the greened double-shell wall was only 0.03 W/m^{2}K. Moreover, the calculation method resulted in the same trend in which the better the U-value of the bare wall, the lower the impact of the greening. The impact of the living wall according to the calculation method ranged from 0.003 to 0.17 W/m^{2}K.

3.3. Impact on heat transport

The impact of the living wall on the heat and moisture transfer through the facade differs according to the season and the day/night cycle. To demonstrate these differences and to allow for close analysis of the results, the simulation outputs were sorted into four groups: summer days, summer nights, winter days, and winter nights. Summer and winter seasons were defined according to summer and winter solstices in the northern hemisphere; day and night hours were defined as the shortest day or night period within the season in question at the simulation location (Mannheim, Germany). The results are presented in box and whisker plots in which the whiskers illustrate the default maximum and minimum values defined as 1.5 × the interquartile range.

As illustrated in Figure 7, the living wall drastically influenced the exterior surface temperature of the wall, in all of the investigated wall assemblies. Moreover, the living wall reduced the fluctuations in the exterior surface temperature due to heat storage in the substrate body. Another reason for this pattern is that the substrate boxes were acting as ventilated insulation reducing the radiative and convective losses in the nights and solar gains in the day. The limited surface temperature fluctuations may contribute to mitigate the wear and damage of the exterior building material, and consequently extend the lifespan of the facade. During summer days, the bare wall had a remarkably higher surface temperature compared to the greened wall; the average difference was 7.2 K. Moreover, the temperature range was greatly reduced when the living wall was implemented. The maximum surface temperature of the greened wall was 26.1°C (in the case of the limestone wall). On the other hand, the bare limestone wall reached a temperature as high as 50.9°C. While a minor player in reducing the temperature is the cooling effect of the plants themselves, this reduction is mostly due to the shading effect of the living wall. This explains why the surface temperature of the bare wall was cooler than the greened wall during summer nights. The average surface temperature difference in the summer nights was 5.8 K. The warmer surface temperature at night is resulted from several factors. First of all, the living wall protects the wall from long-wave radiative heat exchange with the cold sky, hence, increasing its surface temperature. Moreover, the living wall was shielding the wall from the wind, and thus reducing its convective heat losses. As a result, the living wall increased the facades transfer resistance R_{se}. According to the DIN EN ISO 6946 [38], shielding the facade with highly-ventilated components can increase R_{se} from 0.04 m^{2}K/W to $R_{se} = R_{si} = 0.13$ m^{2}K/W. Similar results were observed in the winter nights, in which the average temperature difference between the greened and bare wall was 6.2 K. This pattern also appeared during winter days when the solar radiation is fairly low. Generally, the better the insulation, the lower the average temperature difference between the greened and bare walls. Thus, in the case of the uninsulated brick wall, the average surface temperature difference was 4 K. On the other hand, the double-

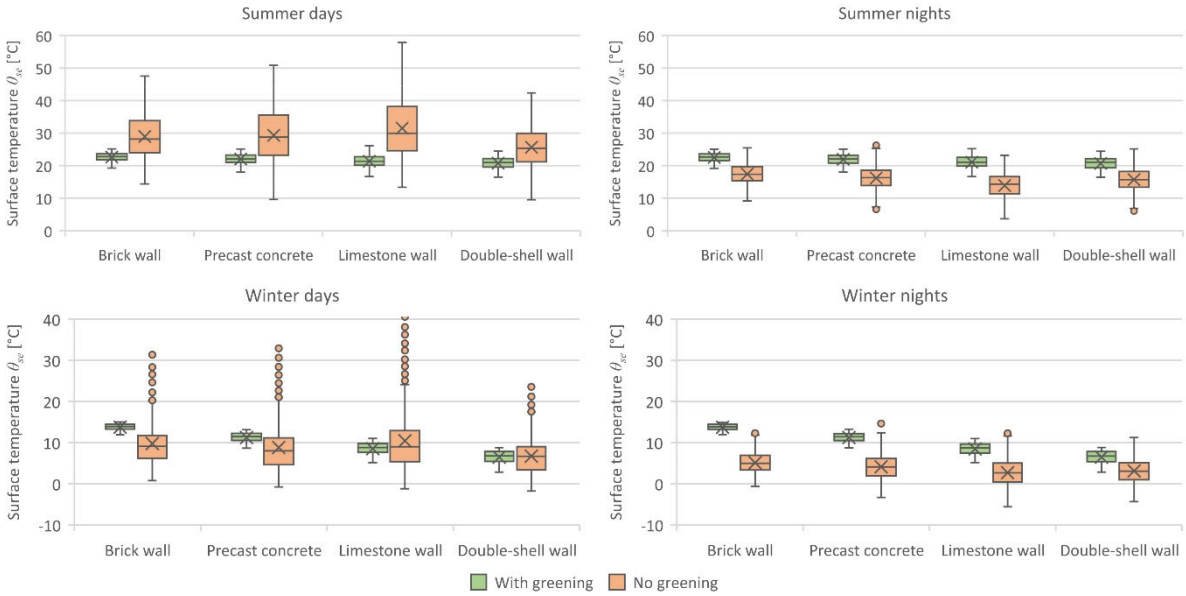

Figure 7. The simulated exterior surface temperature of the investigated wall assemblies

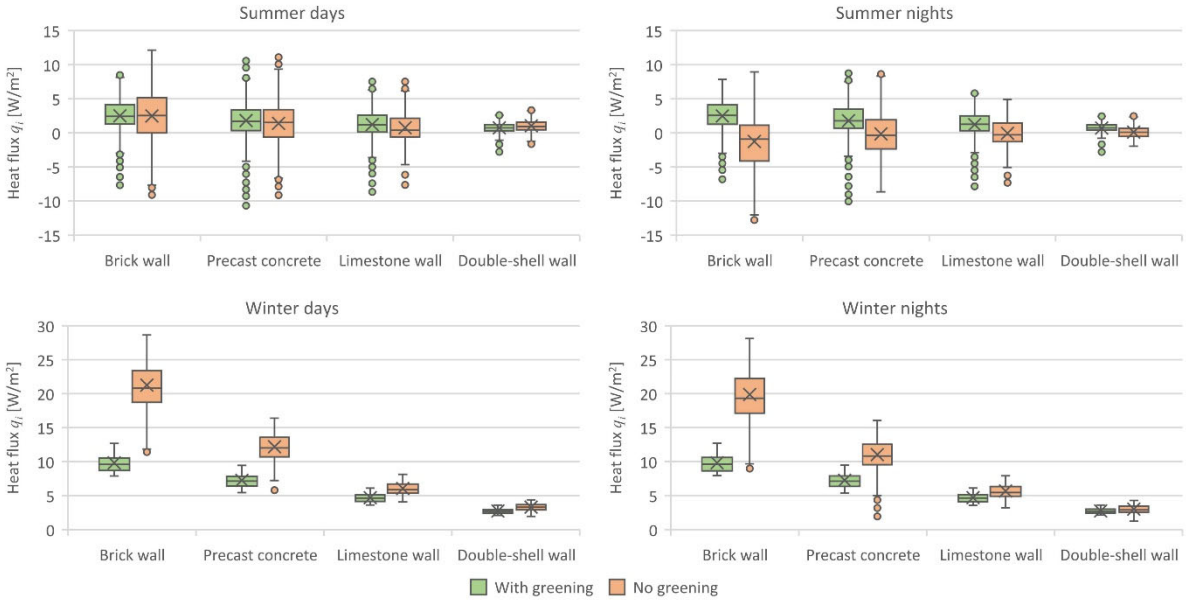

Figure 8. The simulated heat flux through the investigated wall assemblies

shell wall exhibited a difference of only 0.23 K. This is expected as the well-insulated wall prevents heat from leaving the building.

Due to the factors mentioned above, the living wall reduced the heat flux through the wall in the winter (Figure 8). While the average heat flux through the bare wall during the winter days was 10.7 W/m², it was reduced to 6.12 W/m² when the living wall was implemented. This effect was more or less the same during winter nights. The uninsulated brick wall exhibited the largest improvement in heat flux in the wintertime, in which an average of 21.26 and 9.82 W/m² was observed in the cases of bare wall and greened wall, respectively. As the U-value of the wall improves, the impact of the living wall diminishes. In the case of the double-shell wall, the bare wall yielded a wintertime heat flux average of 3.15 W/m² compared to 2.7 W/m² when the greening was used. The enhanced thermal performance agrees with the patterns reported in the literature [5]. The improved thermal envelope suggests an improved energy performance of the building when the living wall is implemented, especially in front of low insulated facades. In the summertime, the living wall reduced the amount of heat entering the building through the wall. The incoming heat is shown in Figure 8 as negative heat flux values. The bare wall allowed a maximum of 12.77 W/m² to enter the building. On the other hand, the wall equipped with greening only allowed a maximum of 10.0 W/m². However, the impact of the living wall on the heat flux during the summer became minimal when the wall insulation improves. The improved thermal performance when the living wall is implemented is also reflected in the

interior surface temperature. This impact can be seen in Figure S1 in the additional supplementary information available in the online version of this article. During the cold wintertime, the living wall increased the minimum interior surface temperature from 16.44°C to 18.43°C. Similarly, the living wall decreased the maximum interior surface temperature during the hot days from 26.54°C to 25.01°C. This suggests an improved thermal comfort in the rooms behind the greening due to the changes in indoor mean radiant temperature.

It is important to point out that in this study, the temperature of the supplied greywater was assumed to be equal to the outdoor air temperature. However, in reality, the greywater should be collected in a tank before it is pumped into the living wall for treatment. Since this tank is most likely weather-protected in the unheated basement along with the pumps and other building systems, the greywater temperature will be warmer than the outside air as the winter air temperature in such basements is nearly 10-15°C in Germany. Similarly, the water temperature will be cooler in the summer. Therefore, it is expected that in reality, the investigated living wall will have an even better impact on the thermal performance of the facade compared to the results reported above. Yet, as the temperature of greywater reaching the substrate depends on multiple factors such as the location of the living wall and the length of the pipelines, it is difficult to predict the water temperature in the system. Therefore, this study adapted the worst-case scenario in which the water gained the outdoor temperature before reaching the substrate.

3.4. Impact on moisture transport

Although the living wall involved pumping large quantities of water directly in front of the facade, the relative humidity of the exterior surface was not always higher when the living wall is implemented (Figures 9). During the summer days and due to elevated surface temperature, the relative humidity at the exterior surface was always lower at the bare wall as the direct solar radiation dissipated the moisture from the wall. This applied for all the four investigated wall assemblies independent from their U-value. The average exterior surface relative humidity of the greened walls during summer days was 65.12% compared to 45.55% at the bare wall. An inversed pattern can be seen during the summer nights due to the absence of solar radiation and cooler surface temperatures. In these cases, the relative humidity of the exterior surface of the greened wall assemblies had an average of 62.58% compared to 71.21% at the bare wall. During winter days, the surface relative humidity correlated to the U-value of the assembly since the relative humidity is directly connected to the temperature. The assemblies with higher (worse) U-values, namely the uninsulated brick wall and the precast concrete plate, had a higher exterior surface humidity in the bare wall case. On the other hand, the limestone wall and the double-shell wall had a lower exterior surface humidity in the bare wall case. During the winter nights, both greened and bare double-shell walls had a fairly similar surface relative humidity, while the other three wall assemblies showed a reduced surface relative humidity when greening is used. However, in the wintertime as well as in the summertime, the bare wall cases always illustrated a much larger range and fluctuations in the simulated surface humidity. The surface relative humidity of the bare wall reached a maximum of 99.72% observed on a summer day on the precast concrete plate, while the greened wall never exceeded 93.81%, which occurred on the double-shell wall on a summer day as well. This indicates an improved hygrothermal performance due to the living wall.

Similar patterns can be seen in the moisture content in the simulated walls (Figure 10). When comparing the bare wall cases to each other, the moisture content values differed greatly depending on the physical properties of the wall material (vapour resistance, porosity, etc.). Yet, when focusing on the impact of the living wall on the moisture content, the results depended mainly on the season and the U-value of the wall. During the summertime, the moisture content in the greened wall was always slightly higher regardless of the investigated wall. On average, the greened wall cases resulted in 0.22 kg higher moisture content compared to their bare wall equivalent cases during summer days, which corresponds to an increase of 4.33%. During winter, a mostly inversed pattern is shown. The greened cases had an average of 0.23 kg lower moisture content. In the case of the uninsulated brick wall, this average difference is much higher (0.46 kg). The reason why the wall humidity was not drastically increased by elevated humidity from the greening is the back-ventilation between the wall and the greening, which dissipated the moisture before it reached the wall. As for the reduced moisture content during winter, multiple factors may have contributed to this behaviour. A major factor is the protection against driving rain provided by the living wall. Moreover, the improved thermal behaviour reported earlier led to a warmer surface temperature of the exterior layer, and thus prevented condensation on the wall. Another reason is that the air temperature adjacent to the exterior plaster, i.e. the air temperature directly in front of the bare wall and the air temperature in the air gap behind the living wall, is higher in the winter when the living wall was used. The warmer temperature in the air gap is a result of the warmer exterior surface temperature. Therefore, the relative humidity adjacent to the exterior plaster was lower when the living wall was utilized as the warmer air can carry more moisture. This explains the increasing difference in moisture content between the greened and bare cases as the U-value of the assembly increases. Further information about the air temperature and relative humidity in the air gap can be obtained from Figures S2 and S3 in the supplementary material. Furthermore, Figure S4 shows the simulated degree of saturation at the exterior finishing layer of the investigated wall assemblies, which is defined as the percentage of pore space filled with liquid water. Similar trends were identified regarding the difference between summer and winter times and the relationship between the U-value of the assembly and

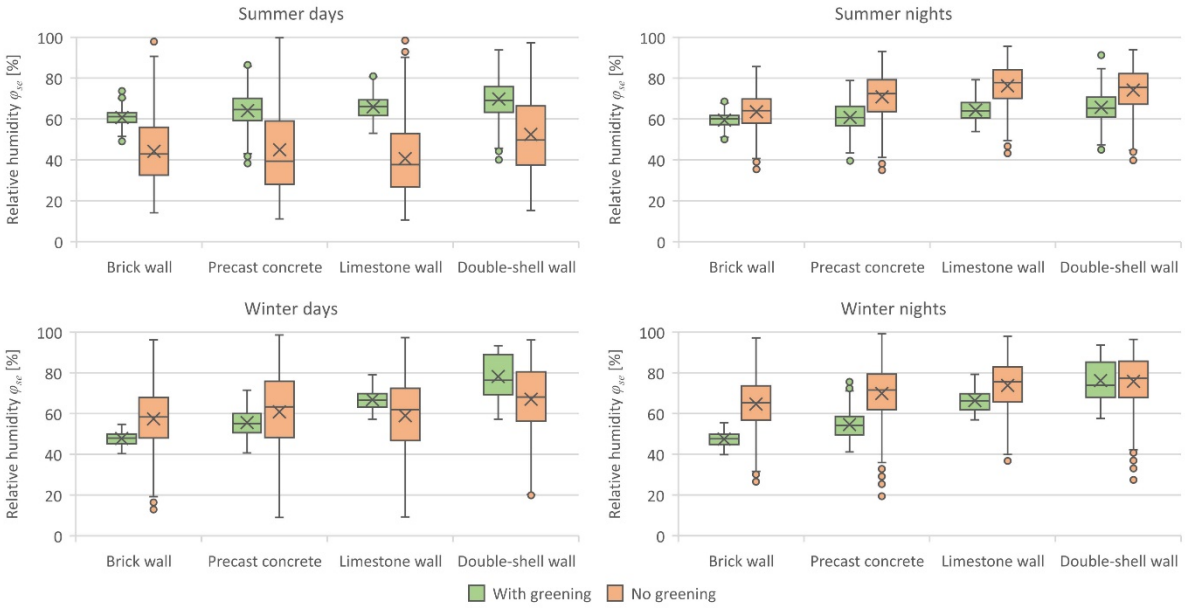

Figure 9. The simulated relative humidity of the exterior surface of the investigated wall assemblies

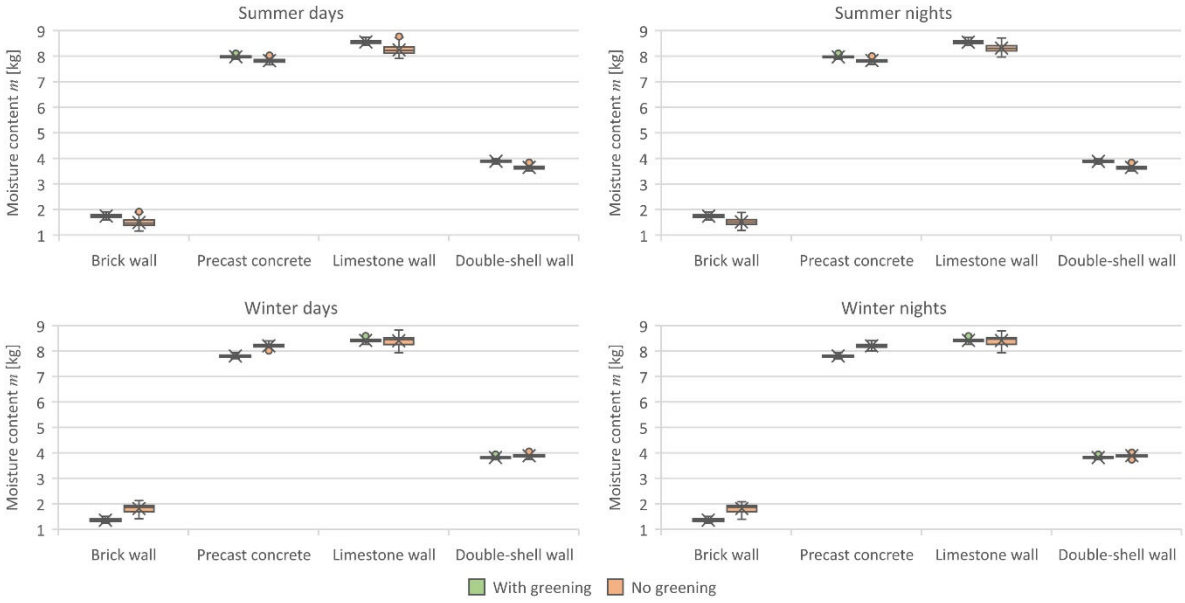

Figure 10. The simulated moisture content in the investigated wall assemblies

the obtained degree of saturation. The reduced moisture in the summertime is due to direct solar radiation heating the wall and drying the accumulated moisture. However, since the risk of moisture is more relevant in winter when the wall cannot dry easily and when cold structures can cause mould and freezing damages, it can be accepted that the living wall generally has a positive impact on the hygrothermal performance of the wall.

Figure 11 presents the condensation risk in the wall throughout the year. The default condensation criterion in the solver was implemented, which is defined as the over-hygroscopic water mass density above 95% relative humidity [22]. The results indicate that the living wall reduced the yearly mass of condensed water to zero in all of the investigated walls. This was due to the combination of warmer structures in the winter and reduced levels of humidity in the wall compared to the bare wall. During the bare wall cases, an elevated condensation mass up to 7.7 kg per year was calculated in the case of the double-shell wall. The other wall assemblies had a yearly condensation mass of 0.55, 1.47, and 2.05 kg in the cases of the uninsulated brick wall, precast concrete plate, and limestone wall, respectively. This indicates a significantly reduced condensation risk in the wall when the living wall is utilized.

4. Conclusions

The hygrothermal performance of a facade equipped with a living wall designated for greywater treatment was simulated. To accurately represent the impact of the plants in

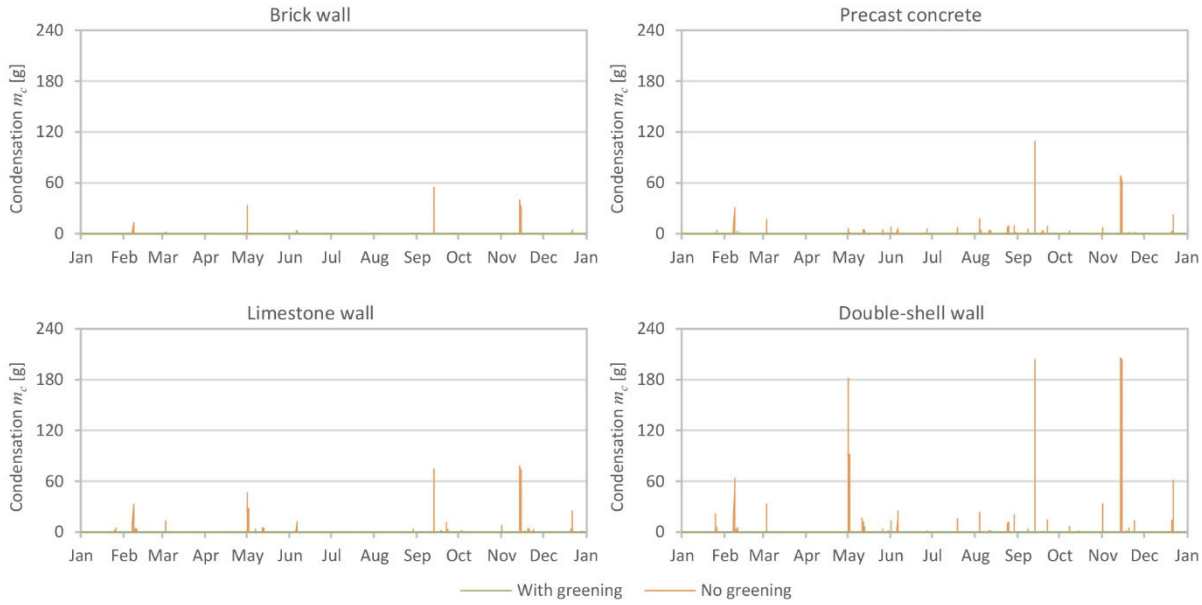

Figure 11. The simulated condensation mass in the investigated wall assemblies

the simulations, ENVI-Met and Delphin were coupled. ENVI-Met simulations showed that the plants remarkably decreased air velocity and received short-wave radiation at the wall. On the other hand, they increased the relative humidity and received long-wave radiation. Air temperature at the living wall illustrated only a slight decrease due to transpirational cooling. However, the plant parameters implemented in this study represented relatively high values of depth and density of the foliage typically used in facade greening. The reason behind this was to investigate cases with a high risk of humidity forming on the wall. Different choices of plants will result in different patterns compared to the results reported in this study.

The hygrothermal simulations conducted with Delphin showed that the living wall can remarkably enhance the effective U-value of the wall assembly. Walls with a high U-value showed the largest improvement of up to 0.77 W/m²K. This improvement was, however, distinctly lower when the bare wall already had a good U-value. In this case, the greening enhanced the U-value by only 0.04 W/m²K (in the case of the double-shell wall). The simulations also showed that the exterior surface temperature and the heat flux through the facade were improved when the living wall was applied. Moreover, the simulations indicated that even with the elevated humidity induced by transpiration and greywater evaporation, the greening improved the moisture content during the cold wintertime and eliminated the risk of condensation in the structure. The impact of the living wall on moisture transport varied among the investigated wall assemblies depending mainly on the season and the U-value of the wall. The presented results are, however, closely related to the boundary conditions and the input data used in the simulations. Assessments conducted using different weather data, different facade orientation, or different wall assemblies will result in deviating findings.

The coupling approach described in this study is highly advantageous especially when investigating greening systems with horizontal substrate containers, i.e. the plants are climbing or trailing directly on the wall. In such cases, the impact of the plants on the wall would be accentuated and the proposed simulation approach will be even more necessary to accurately represent the facade assembly. Moreover, the coupling of Delphin and ENVI-Met is also useful when investigating typical facade constructions (without greening). The advantage of ENVI-Met is that it provides detailed climatic parameters with respect to the building geometry, height, and surroundings. While such parameters strongly influence the physical parameter at the wall, they are typically neglected in hygrothermal simulation tools. However, a major limitation of this approach is the computation time required by ENVI-Met as the coupling requires simulating a whole year to obtain the data required to generate the local climate file. Future research will focus on validating the coupling approach presented in this study. To achieve this, an extensive sensitivity analysis should be first conducted to determine the input parameters that have a significant impact on the output values. This should be conducted for both simulation tools, especially for the parameters that are challenging to measure (e.g. LAD). Afterwards, detailed measurements on a test facade equipped with the investigated living wall should be used to validate the approach.

Acknowledgement

This study was conducted as part of the research project VertiKKA (Vertikale Klimakläranlage zur Steigerung der Ressourceneffizienz und Lebensqualität in urbanen Räumen) funded by the German Federal Ministry of Education and Research (BMBF) as part of the funding initiative Resource-Efficient Urban Districts (RES:Z), Grant No. 033W108G. Their support is appreciated and cherished. We would also like to

thank Bjoernsen Beratende Ingenieure GmbH for coordinating the project and the project research partners for their dedication and enthusiasm. The authors would also like to thank Alina Belinc for her support in conducting the literature review.

Data availability statement

The simulation data are available in the co-submitted Data in Brief article [42].

Declaration of interests statement

The authors declare no conflict of interest.

References

[1] Pérez G, Rincón L, Vila A, González JM, Cabeza LF. Green vertical systems for buildings as passive systems for energy savings. Applied Energy 2011;88(12):4854–9. https://doi.org/10.1016/j.apenergy.2011.06.032.

[2] Bustami RA, Belusko M, Ward J, Beecham S. Vertical greenery systems: A systematic review of research trends. Building and Environment 2018;146:226–37. https://doi.org/10.1016/j.buildenv.2018.09.045.

[3] Perini K, Ottelé M, Fraaij A, Haas EM, Raiteri R. Vertical greening systems and the effect on air flow and temperature on the building envelope. Building and Environment 2011;46(11):2287–94. https://doi.org/10.1016/j.buildenv.2011.05.009.

[4] Susorova I, Angulo M, Bahrami P, Stephens B. A model of vegetated exterior facades for evaluation of wall thermal performance. Building and Environment 2013;67:1–13. https://doi.org/10.1016/j.buildenv.2013.04.027.

[5] Tudiwer D, Korjenic A. The effect of living wall systems on the thermal resistance of the façade. Energy and Buildings 2017;135:10–9. https://doi.org/10.1016/j.enbuild.2016.11.023.

[6] Wong NH, Kwang Tan AY, Chen Y, Sekar K, Tan PY, Chan D et al. Thermal evaluation of vertical greenery systems for building walls. Building and Environment 2010;45(3):663–72. https://doi.org/10.1016/j.buildenv.2009.08.005.

[7] Razzaghmanesh M, Razzaghmanesh M. Thermal performance investigation of a living wall in a dry climate of Australia. Building and Environment 2017;112:45–62. https://doi.org/10.1016/j.buildenv.2016.11.023.

[8] Cheng CY, Cheung KK, Chu LM. Thermal performance of a vegetated cladding system on facade walls. Building and Environment 2010;45(8):1779–87. https://doi.org/10.1016/j.buildenv.2010.02.005.

[9] Chen Q, Li B, Liu X. An experimental evaluation of the living wall system in hot and humid climate. Energy and Buildings 2013;61:298–307. https://doi.org/10.1016/j.enbuild.2013.02.030.

[10] Safikhani T, Abdullah AM, Ossen DR, Baharvand M. Thermal Impacts of vertical greenery systems. Environmental and Climate Technologies 2014;14(1):5–11. https://doi.org/10.1515/rtuect-2014-0007.

[11] Cuce E. Thermal regulation impact of green walls: An experimental and numerical investigation. Applied Energy 2017;194:247–54. https://doi.org/10.1016/j.apenergy.2016.09.079.

[12] Gross A, Maimon A, Alfiya Y, Friedler E. Greywater reuse. Boca Raton: CRC Press; 2015.

[13] Aicher A, Londong J. Development of a living wall system for greywater treatment. Proceedings of the 15th International Specialised Conferences on Small Water and Wastewater Systems, Haifa, Israel 2018.

[14] Prodanovic V, Hatt B, McCarthy D, Zhang K, Deletic A. Green walls for greywater reuse: Understanding the role of media on pollutant removal. Ecological Engineering 2017;102:625–35. https://doi.org/10.1016/j.ecoleng.2017.02.045.

[15] Masi F, Bresciani R, Rizzo A, Edathoot A, Patwardhan N, Panse D et al. Green walls for greywater treatment and recycling in dense urban areas: a case-study in Pune. Journal of Water, Sanitation and Hygiene for Development 2016;6(2):342–7. https://doi.org/10.2166/washdev.2016.019.

[16] Wolcott S, Martin P, Goldowitz J, Sadeghi S. Performance of green wall treatment of brewery wastewater. Environment Protection Engineering 2016;42(4):137–49.

[17] Fowdar HS, Hatt BE, Breen P, Cook PL, Deletic A. Designing living walls for greywater treatment. Water Research 2017;110:218–32. https://doi.org/10.1016/j.watres.2016.12.018.

[18] Capener C-M, Sikander E. Green Building Envelopes – Moisture Safety in Ventilated Light-weight Building Envelopes. Energy Procedia 2015;78:3458–64. https://doi.org/10.1016/j.egypro.2015.11.179.

[19] Horner WE. The damp building effect: understanding needed, not more debate. Annals of Allergy, Asthma & Immunology 2005;94:213–5.

[20] Alsaad H, Voelker C. Heat and moisture transport through a living wall system designated for greywater treatment. Proceedings of BS2021: 17th Conference of the International Building Performance Simulation Association, Bruges, Belgium 2021.

[21] Bruse M, Fleer H. Simulating surface–plant–air interactions inside urban environments with a three dimensional numerical model. Environmental Modelling & Software 1998;13(3-4):373–84. https://doi.org/10.1016/S1364-8152(98)00042-5.

[22] Grunewald J. Documentation of the Numerical Simulation Program DIM3.1", Volume 2: User's Guide. Institute of Building Climatology, Faculty of Architecture, Univesity of Technology Dresden 2000.

[23] Salata F, Golasi I, Vollaro AdL, Vollaro RdL. How high albedo and traditional buildings' materials and vegetation affect the quality of urban microclimate. A case study. Energy and Buildings 2015;99:32–49. https://doi.org/10.1016/j.enbuild.2015.04.010.

[24] Sontag L, Nicolai A, Vogelsang S. Validierung der Solverimplementierung des hygrothermischen Simulationsprogramms DELPHIN. Technical report; Technische Universität Dresden: Dresden, Germany 2013.

[25] Aicher A, Börmel M, Beier S. Grauwasserreinigung an der Fassade. Wasser und Abfall 2020;22(7-8):14–9. https://doi.org/10.1007/s35152-020-0238-1.

[26] Oteng-Peprah M, Acheampong MA, deVries NK. Greywater characteristics, treatment systems, reuse strategies and user perception - a review. Water, air, and soil pollution 2018;229(8):255. https://doi.org/10.1007/s11270-018-3909-8.

[27] DIN 4108-2. Wärmeschutz und Energie-Einsparung in Gebäuden – Teil 2: Mindestanforderungen an den Wärmeschutz (Thermal protection and energy economy in buildings - Part 2: Minimum requirements to thermal insulation). Deutsches Institut für Normung e. V; 2013.

[28] ENVI-Met. ENVI-Met 4: A holistic microclimate model. [June 18, 2021]; Available from: www.envi-met.com.

[29] Qin H, Hong B, Jiang R. Are green walls better options than green roofs for mitigating PM10 Pollution? CFD simulations in urban street canyons. Sustainability 2018;10(8):2833. https://doi.org/10.3390/su10082833.

[30] Huttner S. Further development and application of the 3D microclimate simulation ENVI-met [PhD dissertation]: Johannes Gutenberg-Universität Mainz, Germany; 2020.

[31] Loga T, Stein B, Diefenbach N, Born R. Deutsche Wohngebäudetypologie: Beispielhafte Maßnahmen zur Verbesserung der Energieeffizienz von typischen Wohngebäuden. IWU: Institut Wohnen und Umwelt, Darmstadt, Germany; 2015.

[32] ZUB. Erfassung regionaltypischer Materialien im Gebäudebestand mit Bezug auf die Baualtersklasse und Ableitung typischer Bauteilaufbauten. Zentrum für Umweltbewusstes Bauen e.V; 2009.

[33] MASEA. Materialdatensammlung für die energetische Altbausanierung. [September 13, 2021]; Available from: www.masea-ensan.de.

[34] DIN EN ISO 15927-3. Hygrothermal performance of buildings – Calculation and presentation of climatic data – Part 3: Calculation of a driving rain index for vertical surfaces from hourly wind and rain data; German version EN ISO 15927-3:2009. Deutsches Institut für Normung e. V; 2009.

[35] DIN EN 15026. Wärme- und feuchtetechnisches Verhalten von Bauteilen und Bauelementen – Bewertung der Feuchteübertragung durch numerische Simulation; German version EN 15026:2007 (Hygrothermal performance of building components and building elements - Assessment of moisture transfer by numerical simulation). Deutsches Institut für Normung e. V; 2007.

[36] WTA. Merkblatt 6-2: Simulation wärme- und feuchtetechnischer Prozesse (Simulation of heat and moisture transfer). Wissenschaftlich-Technische Arbeitsgemeinschaft für Bauwerkserhaltung und Denkmalpflege e.V; 2014.

[37] Hauswirth S, Kehl D. Hinterlüftung bei Holzfassaden. Proceedings of the Holzbautag, Biel, Switzerland 2010.

[38] DIN EN ISO 6946. Bauteile - Wärmedurchlass-widerstand und Wärmedurchgangskoeffizient - Berechnungsverfahren (ISO 6946:2017); German version EN ISO 6946:2017 (Building components and building elements - Thermal resistance and thermal transmittance - Calculation methods). Deutsches Institut für Normung e. V; 2017.

[39] ISO 9869-1. Thermal insulation — Building elements — In-situ measurement of thermal resistance and thermal transmittance — Part 1: Heat flow meter method. International Organization for Standardization; 2014.

[40] Wegerer P, Deseyve C, Bednar T. In-situ-Bestimmung thermischer Eigenschaften von Baukonstruktionen. In: Bauphysik-Kalender 2012, Chapter B5 2012:273–96. https://doi.org/10.1002/9783433601235.ch8.

[41] Gromke C, Blocken B, Janssen W, Merema B, van Hooff T, Timmermans H. CFD analysis of transpirational cooling by vegetation: Case study for specific meteorological conditions during a heat wave in Arnhem, Netherlands. Building and Environment 2015;83:11–26. https://doi.org/10.1016/j.buildenv.2014.04.022.

[42] Alsaad H, Hartmann M, Voelker C. Hygrothermal simulation data of a living wall system for decentralized greywater treatment. Data in Brief 2022;40:107741. https://doi.org/10.1016/j.dib.2021.107741

Supplementary material

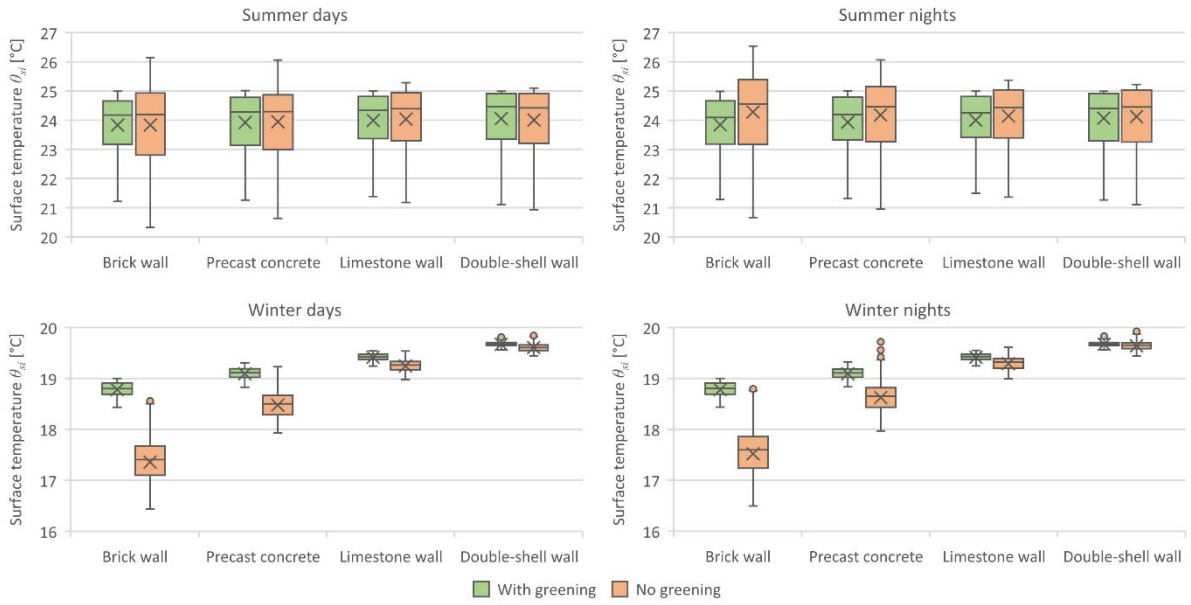

Figure S1. The simulated interior surface temperature of the investigated wall assemblies

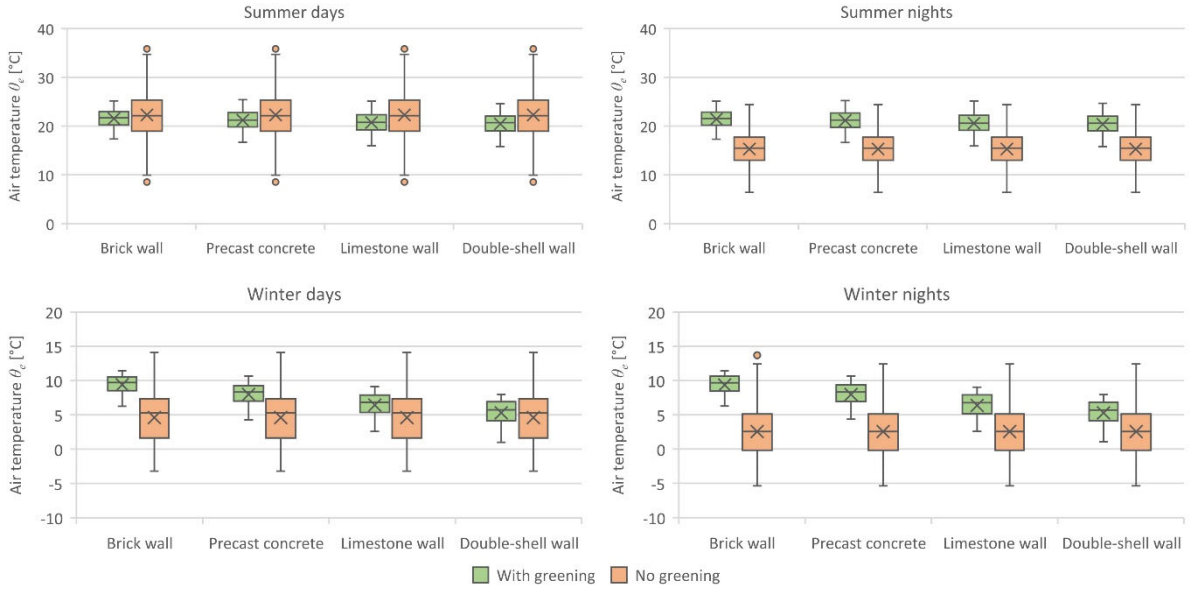

Figure S2. The simulated air temperature adjacent to the wall (in the air gap in the 'with greening' cases and directly in front of the wall in the 'no greening' cases)

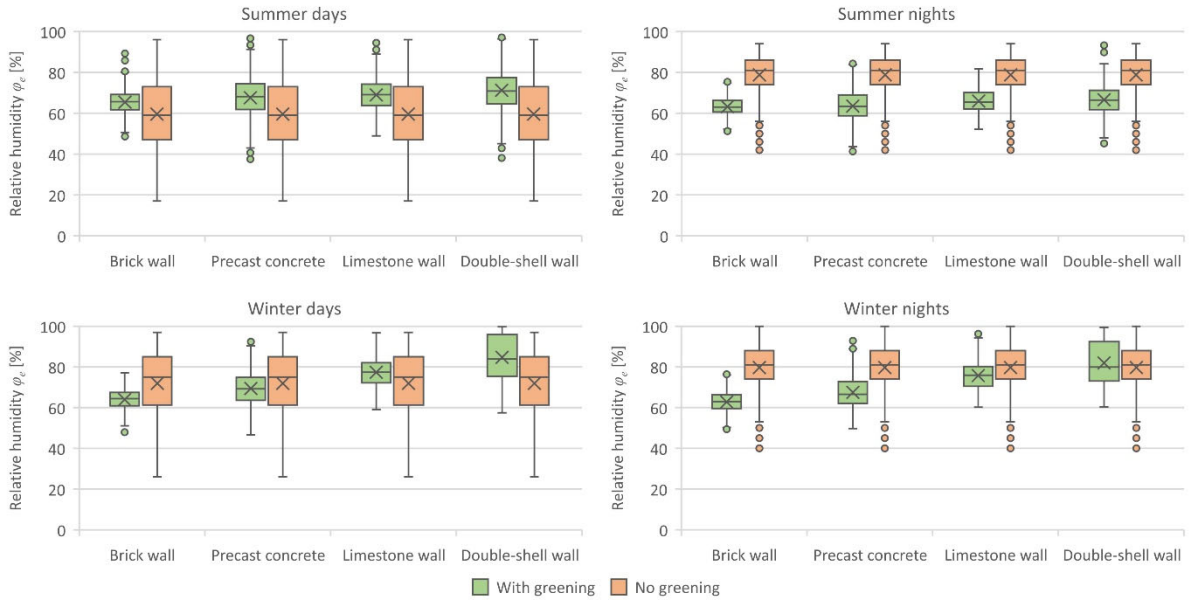

Figure S3. The simulated relative humidity adjacent to the wall (in the air gap in the 'with greening' cases and directly in front of the wall in the 'no greening' cases)

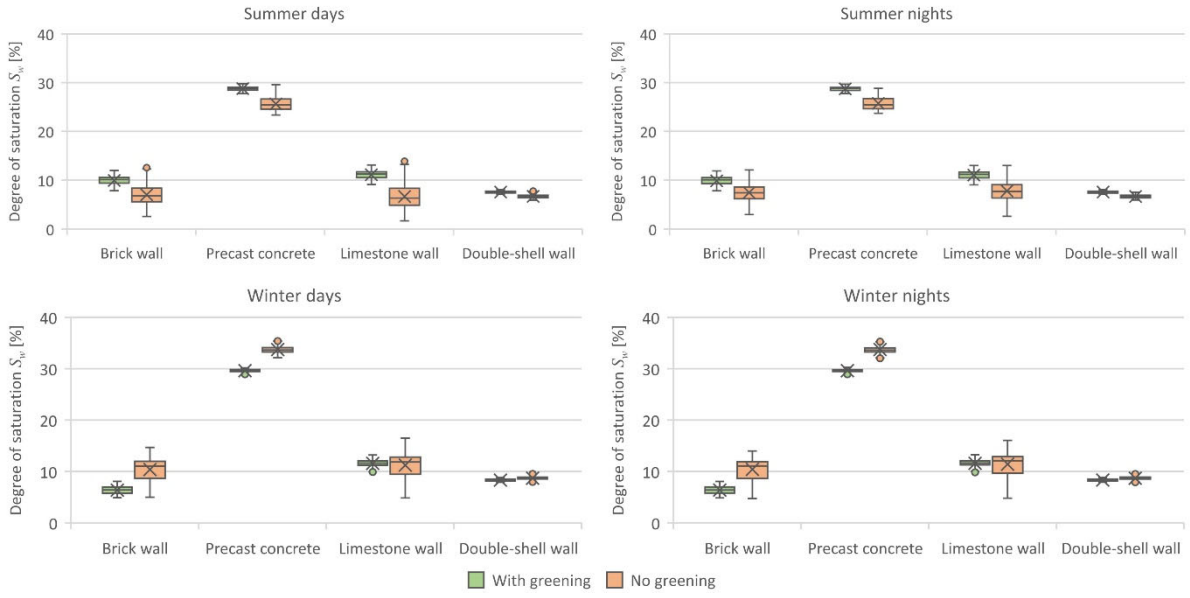

Figure S4. The simulated degree of saturation at the exterior finishes of the investigated wall assemblies